

12-28-1994

## Principles of Semiconductor Surface Reconstruction

C. B. Duke  
*Xerox Webster Research Center*

Follow this and additional works at: <https://digitalcommons.usu.edu/microscopy>



Part of the [Biology Commons](#)

---

### Recommended Citation

Duke, C. B. (1994) "Principles of Semiconductor Surface Reconstruction," *Scanning Microscopy*. Vol. 8 : No. 4 , Article 1.

Available at: <https://digitalcommons.usu.edu/microscopy/vol8/iss4/1>

This Article is brought to you for free and open access by the Western Dairy Center at DigitalCommons@USU. It has been accepted for inclusion in Scanning Microscopy by an authorized administrator of DigitalCommons@USU. For more information, please contact [digitalcommons@usu.edu](mailto:digitalcommons@usu.edu).



## PRINCIPLES OF SEMICONDUCTOR SURFACE RECONSTRUCTION

C. B. Duke\*

Xerox Webster Research Center, 800 Phillips Road, Webster, NY 14580, USA

(Received for publication May 9, 1994 and in revised form December 28, 1994)

### Abstract

Semiconductor surfaces are known to reconstruct, i.e., their surface atomic geometries differ from those of the corresponding surface planes in the bulk material. For clean tetrahedrally coordinated semiconductors, these reconstructed geometries are shown to be predicted by five simple principles. These principles are illustrated by the specific examples of Si(100)-(2x1), Si(111)-(2x1), GaAs(100)-c(2x8), GaAs(111)-(2x2), and relaxed zincblende (110) surfaces. The concept of universal (i.e., material independent) semiconductor surface structures is introduced and shown to be characteristic of the cleavage surfaces of tetrahedrally coordinated compound semiconductors. The role of scanning tunneling microscopy in identifying and validating these principles is highlighted.

**Key Words:** Semiconductor surface structure, scanning tunneling microscopy, Si(100), Si(111), GaAs(100), GaAs(111), GaAs(110), zincblende(110).

### Introduction

It has been recognized since the late 1950s that semiconductors reconstruct: i.e., the positions of the atoms in the top few surface layers exhibit large ( $\approx 1 \text{ \AA}$ ) deviations from their bulk counterparts. The term "reconstruction" is used for surface structures which exhibit a lower symmetry parallel to the surface than the bulk structure. Surfaces for which the atomic positions differ from their bulk values but which retain the symmetry of bulk parallel to the surface are said to be "relaxed". All semiconductor surfaces are either relaxed or reconstructed. Their detailed structures have often been reviewed in the literature (Kahn 1983, 1994; Duke, 1988, 1993b). Our interest herein is why they reconstruct. In particular, we seek general insight into this question which can be used to interpret in a simple, visualizable fashion the enormous body of experimental and theoretical results on specific systems.

To understand why semiconductors reconstruct, we need only two major concepts: chemical bonding and autocompensation. Bulk semiconductors are held together by directional chemical bonds, each of which contains two (spin paired) electrons. Good descriptions of the types and nature of these bonds may be found in Pauling (1960) or Gray (1965). When a surface is formed, these bonds are broken, causing the surface atoms to reposition themselves to form new bonds so that all the electrons on each surface atom are involved in a "saturated" bond containing two electrons. In such a case, one says that the valence of each surface atom is "saturated." For elemental semiconductors, (e.g., Si, Ge), the bonding concept suffices to interpret the broad features of surface reconstructions. For compound semiconductors (e.g., GaAs), however, one also needs a concept which explains the surface chemical compositions (stoichiometry) which can form, since the surface composition is generally not the same as that in the bulk. Autocompensation is this concept. It requires that no net charge accumulates at the surface. It is generally believed that only those surface compositions which satisfy this condition can occur, although a few counterexamples have been proposed in the literature, as discussed later.

\*Address for correspondence:

C.B. Duke  
Xerox Webster Research Center,  
800 Phillips Road, 0114-38D,  
Webster, NY 14580, USA

Telephone number: (716) 422-2106  
FAX number: (716) 265-5080

Thus, we can say that surfaces reconstruct in order to saturate the valences of the surface species subject to the constraint that they are autocompensated.

In order to determine which semiconductor surface structures occur, we need more. In principle, a full quantum mechanical calculation of the surface ground state energy is required to predict equilibrium semiconductor surface structures. Our goal herein is both more modest and more ambitious. We seek to characterize the results of such calculations in terms of simple visualizable "principles" which permit the prediction of chemically feasible (i.e., saturated-bond) structures subject to additional constraints imposed by solid-state effects associated with the one- or two-dimensional nature of surface structures and augmented by the concept of metastability which permits the connection of the structure obtained with the process conditions used to prepare it (Duke, 1993a). This paper is devoted to the articulation of a set of five such principles which permit the interpretation of all known semiconductor surface structures with the possible exceptions of two large-unit-cell structures [Si(111)-(7x7), GaAs(111)-( $\sqrt{19}\times\sqrt{19}$ )]. For these surfaces, the surface chemical bonding has not yet been examined in sufficient detail to determine if these principles suffice to provide a complete interpretation of the observed structure, although efforts have been made to achieve this goal (Chadi, 1991; Brommer *et al.*, 1992; Stich *et al.*, 1992).

Our attention in this paper is focused on the clean low-index faces of tetrahedrally coordinated semiconductors. In the next section, we catalog the structural motifs which occur on these surfaces to produce the observed surface reconstructions. Then, we articulate the five principles of clean semiconductor reconstruction and illustrate each by an example of its application. In the last major section, we indicate some of the major contributions of scanning tunneling microscopy to the determination of surface structures which validate specific aspects of the five principles. We close with a synopsis.

### Surface Structure Motifs

Recognizing that semiconductor surfaces reconstruct or relax to saturate the singly-occupied dangling bonds which would characterize a terminated bulk structure, we regard these surfaces as consisting of new surface chemical compounds which are constrained to fit epitaxially on the bulk substrate. These "epitaxially constrained" (Duke, 1987) surface compounds are typically a few atomic layers thick, thereby forming two-dimensional epitaxial films on the substrate. These films are constructed from a variety of structural elements, which we call motifs. This section is devoted to an articulation of those motifs which have been observed on

tetrahedrally coordinated semiconductor surfaces to date.

Chain structures, roughly analogous to the  $sp^2$  chains found in *trans* polyenes, form on both elemental and compound tetrahedrally coordinated semiconductors. A good example is the  $\pi$  ( $\pi$ )-chain structure found on Si(111)-(2x1) shown in Figure 1. They also are characteristic of the cleavage surfaces of zincblende structure compound semiconductors as shown in Figure 2. An example of such a structure forming spontaneously is afforded by the (111)-(2x2) structure on the cation (111) faces of III-V compounds. As indicated in Figure 3 for GaAs(111)-(2x2), a cation vacancy forms, leaving three dangling As bonds and three dangling Ga bonds. The Ga electrons are transferred to the As species which relax into a cyclic structure analogous to the relaxed chains on the (110) surface. The energy gained by the relaxation of the cyclic chain exceeds that to create the vacancy, leading to a stable structure (Chadi, 1984) which has been observed for GaAs (Tong *et al.*, 1984), GaP (Xu *et al.*, 1985), GaSb (Feidenhans'l *et al.*, 1987) and InSb (Bohr *et al.*, 1985). Therefore, these chain structures, backbonded to the substrate by two bonds for each surface atom, constitute a common structural motif for tetrahedrally coordinated semiconductors.

A second common motif is the surface dimer in which each atom is backbonded to the substrate by two bonds. Common examples are the (2x1) surfaces of Si(100) and Ge(100), shown in Figure 4, and the c(2x8) structures on GaAs(100), shown in Figure 5. This motif permits the surface atoms to saturate their valence by forming a  $\sigma$  bond with its companion and either a  $\pi$  bond between the remaining orbitals (group IV atoms) or two filled non-bonding lone-pair orbitals (group V atoms).

In one case, the (2x2) structure on the As face of GaAs(111), a trimer motif has been found (Biegelsen *et al.*, 1990b). This motif is illustrated in Figure 6.

A fourth common motif is threefold coordinated adatoms on group IV compounds. This is illustrated in Figure 7 for the Si(111)-(7x7) dimer-adatom-stacking fault (DAS) structure (Takayanagi *et al.*, 1985). It also occurs on the Ge(111)-c(2x8) structure (Feidenhans'l *et al.*, 1988). The final observed motif, a stacking fault between the epitaxially constrained surface compound and the bulk substrate, also is illustrated in Figure 7 for the Si(111)-(7x7) structure.

The five motifs illustrated in Figures 1-7 provide the structural elements known to occur to date on the surfaces of clean tetrahedrally coordinated semiconductors. These motifs are formed by atoms in the epitaxially constrained surface compounds to saturate the valences of the atomic constituents in these compounds. The principles governing the formation of these motifs in specific cases are articulated in the following section.

Si (111)-2x1

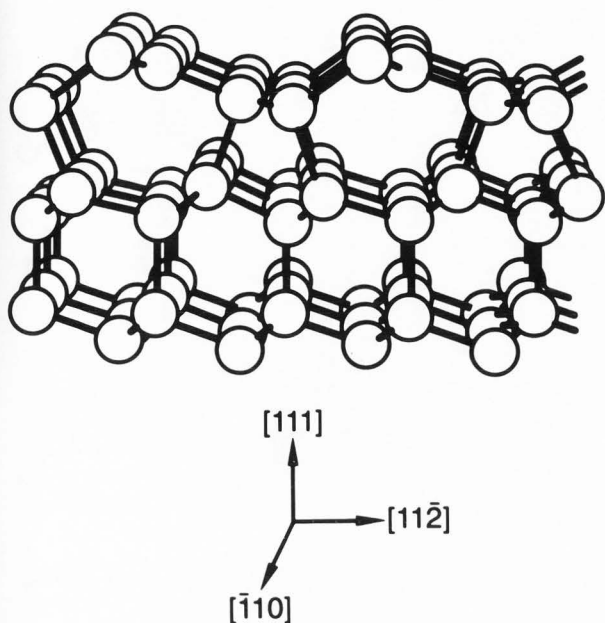


Figure 1. Ball-and-stick model of the (2x1) pi-bonded chain structure on Si(111) resulting from the single-bond-scission cleavage of silicon. [Adapted from Haneman and Chernov, 1989].

GaAs(111) - (2x2)

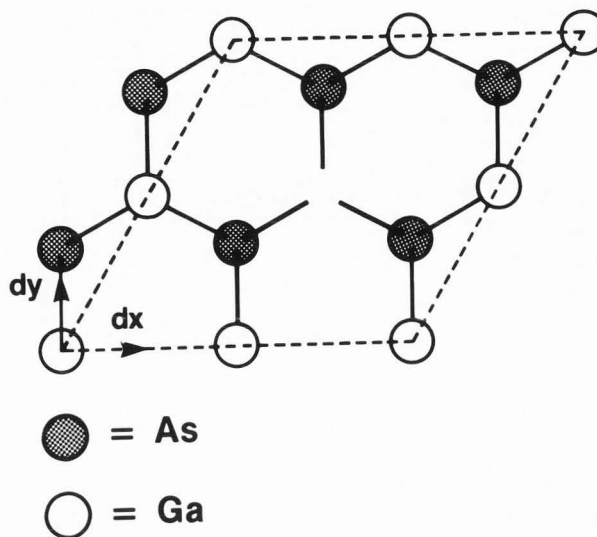


Figure 3. Schematic indication of the ideal (unrelaxed) GaAs(111)-p(2x2)-Ga vacancy structure. [From Duke, 1988].

Zincblende (110)

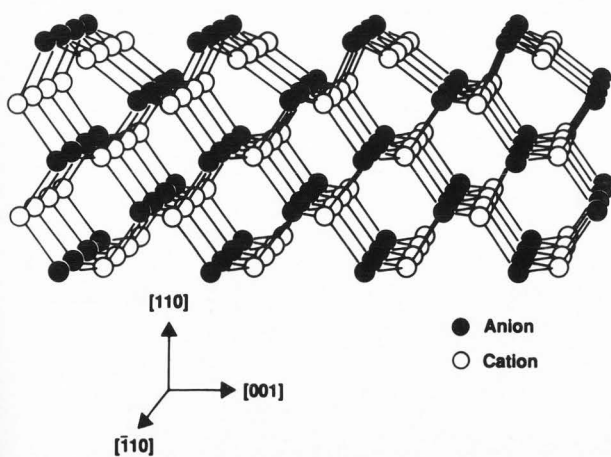


Figure 2. Atomic geometry of the relaxed non-polar (110) cleavage faces of zincblende structure binary compound semiconductors. [Adapted from Duke and Wang, 1988b].

Si (100) - (2 x 1)

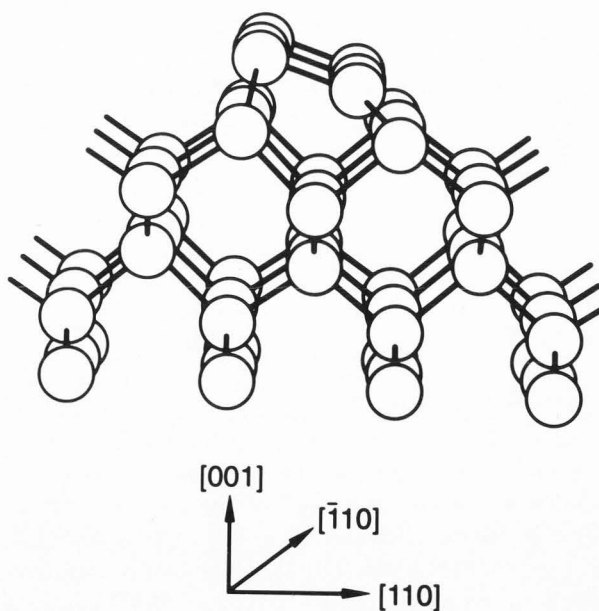
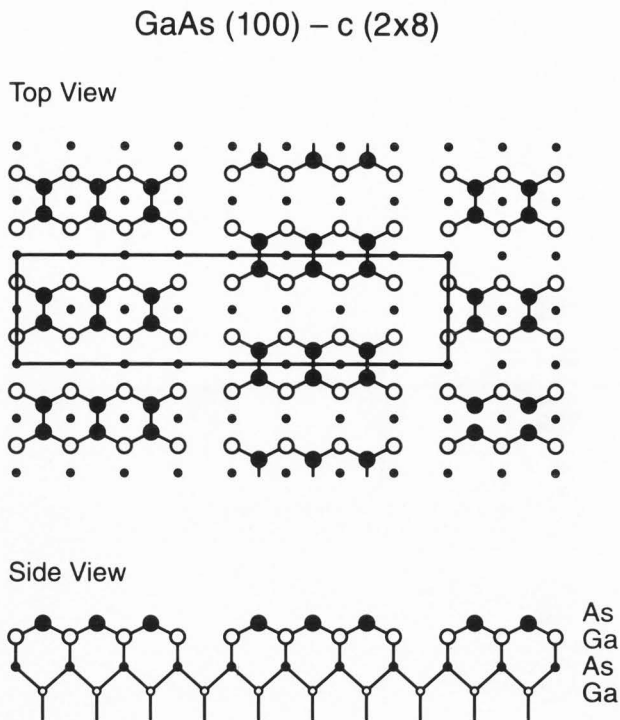


Figure 4. Ball-and-stick model of the buckled dimer structure of Si(100)-(2x1). [Adapted from MacLauren *et al.*, 1987].



**Figure 5.** Schematic illustration of the GaAs(100)-c(2x8) [or (2x4)] reconstruction. The rectangle indicates the surface unit cell. [Adapted from Biegelsen *et al.*, 1990a].

### Principles of Clean Semiconductor Surface Reconstruction

As noted earlier, a useful conceptual model of semiconductor surface reconstruction is afforded by the recognition that the atomic geometry of the uppermost few atomic layers is driven by chemical forces which tend to saturate the valences of the atomic species in these layers. If chemical bonds are formed in this process, the energy gain per bond per atom may be substantial (e.g.,  $\Delta E \approx 1$  eV) (Chadi, 1989). These bonds form a new surface compound which places the substrate under elastic stress. Hence, the substrate atoms relax to new equilibrium positions. The energy gain in this relaxation is about 0.01 eV/surface atom (Chadi, 1979b; Duke, 1993a). We envisage semiconductor surface reconstructions as occurring via the formation of a new "epitaxially constrained" chemical compound on the surface ( $\Delta E \sim 1$  eV/atom) together with the local atomic elastic relaxation of the substrate ( $\Delta E \sim 0.01$  eV/atom) on which it is "grown" epitaxially (Duke, 1987, 1993a). This section is devoted to the articulation of five "principles" which govern the formation of these epitaxially constrained surface compounds.

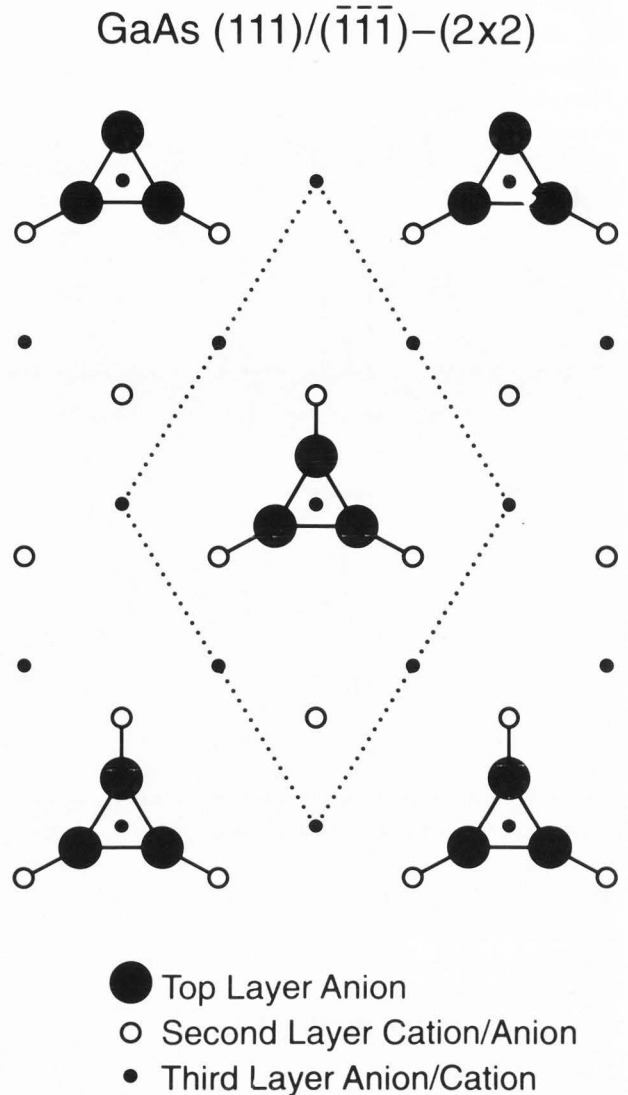


**Figure 6.** Schematic illustration of the trimer model of the GaAs(111)-(2x2) and GaAs( $\bar{1}\bar{1}\bar{1}$ )-(2x2) reconstructions. Large solid circles denote top layer As atoms in the "trimer". For GaAs(111)-(2x2), small open circles designate top-layer Ga atoms and small solid circles denote second layer As atoms. For GaAs( $\bar{1}\bar{1}\bar{1}$ )-(2x2), small open circles designate top-layer As atoms and small solid circles denote second-layer Ga atoms. [Adapted from Biegelsen *et al.*, 1990b].

**Principle (1):** Reconstructions tend either to saturate surface "dangling" bonds via rehybridization or to convert them into non-bonding electronic states.

On the (100) faces of both elemental and compound semiconductors, dimers form to saturate the valences of the surface atoms. The simplest examples are the (100)

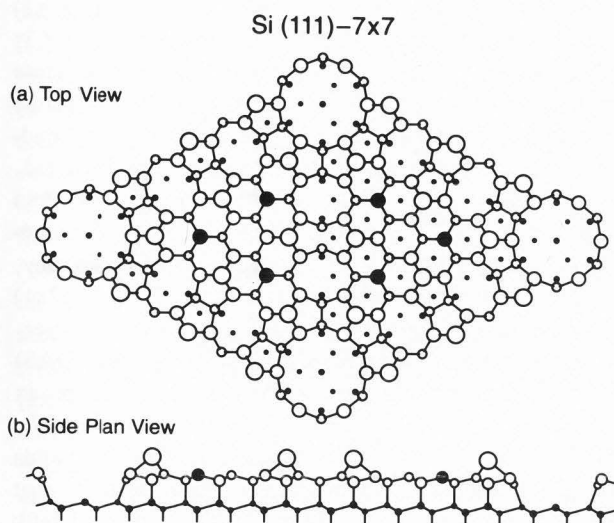


**Figure 7.** Schematic illustration of the top [panel (a)] and side [panel (b)] views of the dimer-adatom-stacking fault (DAS) model of the Si(111)-(7x7) structure. The side view is given along the diagonal of the unit cell. In the top view [panel (a)], the large shaded circles designate the adatoms in the top layer of the structure. The large solid circles designate "rest atoms" in the second layer which are not bonded to an adatom. Large open circles designate triply bonded atoms in this layer, whereas small open circles designate fourfold coordinated atoms in the bilayer beneath. Smaller solid circles designate atoms in the fourth and fifth bilayers from the surface. The size of all circles is proportional to the proximity to the surface. The side view [panel (b)] is a plan view of nearest-neighbor bonding in a plane normal to the surface containing the long diagonal of the surface unit cell. Smaller circles indicate atoms out of the plane of this diagonal. [Adapted from Takayanagi *et al.*, 1985].

surfaces of Si and Ge, for which the (2x1) surface structures consist of rows of dimers. These structures are illustrated in Figure 4. These dimers form to saturate the valences of the two Si or Ge surface species. A sigma ( $\sigma$ ) and a pi ( $\pi$ ) bond forms between the two atoms in each dimer. Thus, one can envisage the two dangling bonds of the bulk-terminated surface as being saturated by the participation of the associated electrons in these two bonds. Detailed accounts of this bonding scheme may be found in the literature (Chadi 1979a; Ihm *et al.*, 1980; Yin and Cohen, 1981).

On the (111) surfaces of Si and Ge,  $\pi$ -bonded chains, analogous to polyene bonding in organic compounds, occur to saturate the valences of the surface

atoms (Pandey, 1981, 1982). These are illustrated in Figure 1. In this case also, the electrons in the two dangling bonds of the unrelaxed bulk surface participate in one  $\sigma$  and one  $\pi$  bond. Unlike the dimer motif on Si(100)-(2x1), which leads to localized dimer  $\pi$ -bonding, however, the  $\pi$ -chain motif leads to delocalized  $\pi$ -electron bonding all along the chain. The energetics of both motifs reveal that they occur because they stabilize the resulting epitaxially constrained surface compound by virtue of involving all the bulk-terminated dangling bond electrons in surface bonds (Ihm *et al.*, 1980; Yin and Cohen, 1981; Pandey, 1981, 1982).

The tilted chains on zincblende III-V (110) surfaces, illustrated in Figure 2, are reminiscent of the  $\pi$ -bonded chains of the (2x1) structures on Si and Ge(111). Like the  $\pi$ -bonded chains, they are stabilized by the requirement that the surface atoms saturate their valences. The microscopic mechanism for their stability is, however, slightly different, being associated with charge transfer from the surface cation to the surface anion and subsequent rehybridization of the surface bonds to achieve the most stable bonding configuration of the resulting two-dimensional epitaxially-constrained surface compound (Duke, 1988, 1992). In this case, the unoccupied cation states are raised in energy by the relaxation because the group III cation bonds in a saturated  $sp^2$  local environment. They become non-bonding  $\pi$ -states associated with the  $sp^2$  bonded cations. Similarly, the doubly occupied anion "dangling bond" states are lowered in energy and converted to non-bonding electronic states characteristic of saturated ( $s^2p^3$ ) bonding of group V elements in molecules. Therefore, for III-V compounds, the tilting of the surface chains is an excellent illustration of **Principle (1)**. Details of the character of the various surface bonding and antibonding electronic states are described, e.g., by Mailhiot *et al.* (1985). For II-VI compounds, the situation is more complex (Duke and Wang, 1989), so we need to extend **Principle (1)** as described in connection with **Principle (5)**, below.

**Principle (2):** In many cases (and all quasi-one-dimensional ones), surfaces can lower their energies by atomic relaxations leading to semiconducting (as opposed to metallic) surface state eigenvalue spectra.

As emphasized earlier, the epitaxially constrained surface compounds on clean tetrahedrally coordinated semiconductor surfaces are two-dimensional layer compounds whose behaviors are governed in detail by solid-state phenomena. Our five principles are designed to predict and interpret only the local structural motifs which occur. Thus, long-range broken symmetry states (e.g., the conversion of the (1x2) states on Si(100) (Garcia and Northrup, 1993) and Ge(100) (Needels *et al.*, 1988) into c(4x2) states at low temperature) and the

occurrence of steps (Alerhand *et al.*, 1988) are phenomena whose description lies beyond these principles. Nevertheless, cases occur in which solid state effects influence the local structural motifs. The lowering of the surface energy by virtue of a metal-to-insulator transition for electrons in surface states accompanied by a structural transition is one of those cases. Hence, it is encompassed in our set of five principles by virtue of **Principle (2)**.

An example of this principle is given by the tilted dimer (2x1) structures of the (100) surfaces of Si and Ge shown in Figure 4. From a chemical perspective, we can regard the surface dimer in Figure 4 as being bound by a  $\sigma$  bond emanating from the two dangling bond orbitals in between the dimerized surface atoms and a weaker  $\pi$  bond emanating from the two dangling bond orbitals pointed away from the dimer. The associated  $\pi^*$  bonding orbital is empty but is separated from the bonding orbital by only a small energy gap ( $E_g \sim 0.5$  eV) (Chadi, 1979a; Ihm *et al.*, 1980). On the surface, the molecular  $\pi$  and  $\pi^*$  orbitals broaden into bands associated with the wave vectors in the surface Brillouin zone. These bands overlap for a symmetric (i.e., untilted) dimer, so that the surface becomes metallic. Since these bands are nearly one-dimensional (along the rows of dimers), however, it is energetically favorable for the surface to lower its energy by an atomic relaxation (Yin and Cohen, 1981; Duke, 1993a), and hence, the dimers tilt, opening up a gap between filled electronic states originating primarily from the "up" atom and empty states originating primarily from the "down" atom. The resulting "asymmetric" or tilted dimer model is in good quantitative accord both with experimental determinations of the surface excitation spectra (Uhrberg and Hansson, 1991; Northrup, 1993) and with modern (i.e., converged) total energy calculations (Dabrowski and Scheffler, 1992; Krüger and Pollmann, 1993).

**Principle (3): Cleaved surfaces yield minimum-energy geometries if, and only if, the pathway to these surfaces from the bulk structure exhibits an activation energy less than or comparable to  $\kappa T$ , where  $\kappa$  is Boltzmann's constant and  $T$  is the cleavage temperature. More generally, the surface structure observed will be the lowest energy structure kinetically accessible under the preparation conditions.**

This principle is required to describe the well-known result that for surfaces prepared by molecular beam epitaxy (MBE) or even ion-bombardment and anneal cycles the surface structure obtained depends on the process sequence used to obtain it. A particular example illustrated by the structural motifs in Figures 1 and 7 is the (111) surface of Si. When cleaved at "low" temperatures (i.e.,  $T \leq 350^\circ\text{C}$ ), a reconstruction of the upper-

most four atomic layers occurs leading to a (2x1)  $\pi$ -chain top-two-layer structure as shown in Figure 3. This structure yields a semiconducting surface state spectrum characterized by a gap between the  $\pi$  and the  $\pi^*$  states of the surface chains. Because of the  $\pi$  bonding along the chains, all the surface bonds are saturated, with the new surface epitaxially-constrained compound consisting of the uppermost two layers of " $\pi$ -bonded-chains" on an elastically distorted Si substrate (Pandey, 1981). But the Si(111)-(2x1) and Ge(111)-(2x1)  $\pi$ -bonded-chains are not the lowest-energy structures. Rather, these are the dimer-atom-stacking fault (DAS) structure shown in Figure 7 for Si(111)-(7x7) or an adatom structure for Ge(111)-c(2x8) (Feidenhans'l *et al.*, 1988). The reason that low temperature cleavage yields the higher-energy (2x1) structure is believed to be that this geometry can be reached from the truncated bulk geometry via a nearly activationless ( $E_a \leq 0.03$  eV) process (Northrup and Cohen, 1982). The DAS and c(2x8) structures require large-scale atomic motions which can be accessed only at high temperatures.

**Principle (4): Surfaces tend to be autocompensated.**

Another aspect of the metastable character of surface structures is that, for compound semiconductors, the surface composition as well as structure can vary with fabrication conditions. An important constraint used to restrict the range of possible surface compositions (stoichiometries) is that no charge accumulate at the surface (Harrison, 1979). Since its initial proposal, this constraint has been developed into a set of electron counting rules which can be used to select structural models which satisfy it (Ludeke, 1977; Farrell, *et al.*, 1987; Pashley, 1989; Chadi, 1991) based on the notion that bonding and non-bonding surface states that lie below the Fermi energy at the surface must be filled whereas antibonding and nonbonding surface states lying above the Fermi energy must be empty. This criterion is referred to as the "nonmetallicity" condition. Surfaces which satisfy it are said to be autocompensated. To describe doped semiconductors, the simple forms of these counting rules must be extended to include charge in the space charge region (Pashley and Haberern, 1991). With these extensions, the autocompensation principle is satisfied by the known surface structures for which a quantitative test is available. It has been proposed to fail in a few cases, e.g., GaAs(111)- $(\sqrt{19} \times \sqrt{19})$  (Biegelsen *et al.*, 1990b), but these cases all consist of large complicated structures for which a detailed description of the surface bonding is not yet available.

This principle describes a remarkable variety of structures on the polar surfaces of compound semicon-

ductors (Pashley, 1989; Biegelsen *et al.*, 1990a, 1990b). It determines a set of allowed stoichiometries for these surfaces and is satisfied trivially for the 1:1 non-polar cleavage faces. While this principle does not predict the detailed atomic geometry, it does identify candidate structures from which a possible geometry ought to be selected. Thus, for example, it predicts both the 3:1 ratio of anion dimers to missing anion dimers on III-V (100) as shown in Figure 5 (Pashley, 1989; Biegelsen *et al.*, 1990a), the 2:2 ratio of anion to cation dimers observed when the Ga in the second layer also dimerizes (Northrup and Froyen, 1993), the change to a uniform (2x1) dimer structure on II-VI (100) (Pashley, 1989), and a further change to a c(2x2) adatom (or vacancy) structure for I-VII (100) (Dassanayake *et al.*, 1993). It also is pertinent to the (111) surfaces, for example, the cation vacancy structure characteristic of III-V (111)-(2x2) shown in Figure 3 (Chadi, 1989) and the anion trimer structure exhibited by III-V (111)-(2x2) shown in Figure 6 (Biegelsen *et al.*, 1990b). The counting-rule version of the autocompensation principle has been applied to describe allowed surface structures on III-V (100) surfaces for many years (Appelbaum *et al.*, 1976; Ludeke, 1977). Detailed microscopic calculations on GaAs(100) also support its validity (Appelbaum *et al.*, 1976; Northrup and Froyen, 1993).

**Principle (5):** For a given surface stoichiometry, the surface atomic geometry is determined primarily by a rehybridization-induced lowering of the surface-state bands associated with either surface bonds or (filled) anion dangling bond states.

Whereas, for compound semiconductors, **Principle (4)** determines allowed surface stoichiometries, **Principle (5)** determines the detailed atomic geometry. It is formulated as an extension to arbitrary surfaces of arbitrary compound semiconductors of **Principle (1)** which in its articulated form is most useful for the non-polar surfaces of group IV and III-V semiconductors. It is an extension for both non-polar and polar surfaces because it embodies a new notion not contained in **Principle (1)**: that of surface chemical bonding carried by the delocalized electronic surface states characteristic of a two-dimensional epitaxially-constrained surface compound. This is an extension of traditional local bonding concepts characteristic of molecular bonding (Gray, 1965) and bulk solid (Pauling, 1960) bonding which is required by similarities between the cleavage surface bonding of III-V and II-VI semiconductors (Duke, 1992). Thus, **Principle (5)** can be applied simply to describe the relaxations of the cleavage faces of II-VI semiconductors whereas **Principle (1)**, while still true, does not illuminate the cause of the resulting surface structures.

The fundamental motivation for developing **Principle (5)** as an extension to **Principle (1)** is the recognition (Duke, 1983) that the (110) cleavage surface structures of all zincblende structure compound semiconductors are essentially identical when distances are measured in units of the bulk lattice constant. Since the coordination chemistry of II-VI compounds differs greatly from that of III-V's, local coordination chemistry concepts like those articulated in **Principle (1)** had to be recast into the more general context of **Principle (5)**. The verification of **Principle (5)** for the cleavage faces of both wurtzite and zincblende II-VI and III-V compounds has been reviewed recently by Duke (1992).

For the zincblende cleavage faces, the surface structure scaling rules have been extended to develop the more general notion of universality for the potential energy surfaces governing the relaxation and lattice dynamics of these surfaces (Duke, 1992; Godin *et al.*, 1992). The minima in these surfaces specify the relaxed atomic geometries whereas their curvature in the vicinity of these minima specify the effective atomic dynamics spring constants in the vicinity of the surface (and hence the phonon frequencies). The existence of the scaling laws predicted by these potential energy surfaces confirms the concept that the constraint of epitaxy with the tetrahedrally-coordinated substrate leads to new types of surface chemical bonding, mediated by delocalized two-dimensional surface states rather than by local charge densities, relative to molecular coordination chemistry. **Principle (5)** is the articulation of this result that surface states rather than local bonds are the mediators of the bonding in epitaxially constrained surface compounds, specifically those occurring at clean surfaces.

**Principle (5)** has not been tested rigorously for surfaces other than the zincblende and wurtzite cleavage surfaces. Since all of the new motifs characteristic of epitaxially constrained surface chemical bonding are localized within a few atomic layers of the surface, their bonding and occupied non-bonding charge densities must, by definition, be comprised of linear superpositions of electronic eigenstates which are surface states or resonances. Energy minimization calculations (Chadi, 1984; Brommer *et al.*, 1992; Dabrowski and Scheffler, 1992; Stich *et al.*, 1992; Krüger and Pollmann, 1993; Northrup and Froyen, 1993) typically do not identify the surface state contributions to the total energy. Hence, the microscopic origin of the energy lowering by virtue of the surface relaxations usually is not explored. Only for the cleavage faces of zincblende (Mailhot *et al.*, 1985; Duke and Wang, 1989; Duke, 1992) and wurtzite (Duke and Wang, 1988a, 1988b, 1989) has the separation of the surface state energies been made explicitly, so that **Principle (5)** can be validated. **Principle (5)** is, however, expected to be valid for all surfaces of tetra-



hedrally coordinated semiconductors, reducing in some cases to **Principle (1)** which is more visualizable in terms of traditional local chemical bonding concepts.

### Role of Scanning Tunneling Microscopy

Since this paper was delivered at The 1994 Scanning Microscopy Meeting, the purpose of this section is to indicate a few highlights of the role of scanning tunneling microscopy (STM) in testing and validating the five principles of clean surface reconstruction. This section is not intended to be a comprehensive review of STM studies of semiconductor surfaces (a subject which currently encompasses nearly 1000 papers). Rather, it describes the author's impression of a few key results which bear directly upon the principles articulated above.

Historically, the first of these is the imaging of the Si(111)-(7x7) structure by Binnig *et al.* (1983). This study confirmed directly the (7x7) character of the surface unit cell as well as revealed the existence of both the twelve adatoms per unit cell and the deep holes at the corners of the unit cell evident in the DAS structure illustrated in Figure 7. It did not determine a quantitative surface structure, which was first accomplished by Takayanagi *et al.* (1985) using transmission electron diffraction via an analysis leading to the initial proposal of the DAS structure. Subsequent STM studies of clean Si(111)-(7x7) focused on exploring the nature of the associated electronic surface states by studying the bias dependence of the STM images as well as various measures of the current-voltage spectra at fixed tip positions. One consequence of this effort was a quantitative validation of the DAS model relative to other proposed models (Tromp *et al.*, 1986). A second was the recognition that STM images the electronic surface states of Si(111) rather than atomic positions per se (Hamers *et al.*, 1986a, 1987). Images of the adatoms as found by Binnig *et al.* (1983) require the selection of a voltage at which the electrons in surface states localized on the adatoms contribute predominately to the tunneling current.

The intimate connection between surface electronic and geometrical structure in generating STM images is emphasized by studies of the zincblende (110) surfaces. In this case, if the sample is biased positively relative to the tip, electrons flow from the tip into empty cation (e.g., Ga) derived states, whereas if it is biased negatively electrons flow from filled anion (e.g., As) derived states into empty states in the tip. Thus, at (moderate  $V_a \sim 2V$ ) positive bias the cation sublattice is imaged whereas at negative bias the anion sublattice is imaged (Feenstra *et al.*, 1987). Only via a synthesis of the cation and anion selective images is the chain motif shown in Figure 2 revealed. Such superpositions can be ana-

lyzed to estimate the lateral separation between the cation and anion sublattice. Moreover, if the relaxation is taken to be bond-length-conserving, which is the case for highly covalent compound semiconductors like GaAs and InSb (Duke, 1992), then the measurement of this lateral displacement also determines the tilt angle of the chain, and hence, the vertical cation-anion displacement. This method of analysis has been used to validate prior structure determinations [mostly via low energy electron diffraction (LEED)] for both GaAs(110) (Feenstra *et al.*, 1987) and InSb(110) (Whitman *et al.*, 1990). These analyses also reveal two additional aspects of structure estimates via STM imaging. First, the images depend sensitively on the electronic surface states as well as on atomic positions, so that even the qualitative features of the images reflect the behaviour of the surface-state wave functions rather than the surface atomic geometry alone. Second, in part because of the mixing between electronic and atomic information in the images and in part because of the implicit dependence of these images on the tip, the uncertainties in the estimated structural parameters are large ( $\Delta d \approx 0.4 \text{ \AA}$  in these cases) relative to  $0.1 \text{ \AA}$  or less for LEED and ion-scattering studies (Duke, 1988). The STM images, while marvelously informative about qualitative features of surface structure and topography, are of limited utility for quantitative surface structure determination.

STM studies of the (2x1) reconstruction of the (111) and (100) surfaces of Si and Ge move still further from determinations of atomic geometry to measures of surface electronic structure. Early studies of Si(111)-(2x1), while unable to image atomic structure within the  $\pi$ -bonded chains, were able to distinguish between the  $\pi$ -bonded chain model and a previously proposed buckling model for the surface structure (Feenstra *et al.*, 1986). Subsequent studies yielded improved images in which structure within the chains could be resolved, but which was shown to be associated with the features of the wave functions of the  $\pi$  and  $\pi^*$  states accessed by the tunneling electrons (Feenstra and Stroscio, 1987; Stroscio *et al.*, 1987). Specifically, by imaging separately states at the bottom of the (unoccupied)  $\pi$  band and the top of the (occupied)  $\pi$  band the two inequivalent Si atoms in the chain could be imaged separately, just like the cation and the anion in the analogous chains in the zincblende (110) surface. The electronic inequivalence of the two Si species in the Si(111)-(2x1)  $\pi$  bonded chains renders them analogous to the anion and cation, respectively, on zincblende (110). Hence, just as for zincblende (110), imaging of the surface atomic geometry requires the superposition of images taken at different bias voltages selected such that all of the surface species are observed for at least one of the voltages.

STM studies of Si(100)-(2x1) followed the same

general trend as those of Si(111)-(2x1). Early work led to the confirmation of the dimer model (Tromp *et al.*, 1985; Hamers *et al.*, 1986b), with later studies leading to the recognition that the details of the images reflected the electronic structure of the  $\pi$  and  $\pi^*$  states of the dimer rather than the total charge density outside the surface (Hamers *et al.*, 1987). Another complication occurs for Si(100)-(2x1), however, associated with the dynamics of the dimers. An isolated dimer can switch from one atomic component up to its antisymmetric equivalent with the other atom up on rapid time scales because of the low ( $E_a \approx 90$  meV) energy barrier for this interconversion process (Weakliem *et al.*, 1990; Kochanski and Griffith, 1991; Dabrowski and Scheffler, 1992). Therefore, at room temperature, STM measures only the time average of this process, which is a symmetric dimer unless a neighboring defect quenches the interconversion by rendering the two degenerate dimer states inequivalent. After years of controversy over whether the symmetric or tilted dimer constitutes the lowest-energy state, this issue seems to have been resolved experimentally by the measurement of the freezing in of the asymmetric dimer states at low ( $T = 120$  K) temperatures (Wolkow, 1992). Thus, the identification of the tilted dimer structure shown in Figure 4 as the appropriate atomic motif for Si(100)-(2x1) (and lower symmetry low-temperature states as well), seems secure.

In contrast to the situation for the low-index faces of Si and the non-polar faces of tetrahedrally-coordinated compound semiconductors, for which STM has largely confirmed surface structures previously determined by other methods, for the polar surfaces of compound semiconductors, STM has led the way in establishing surface structural motifs. GaAs(100) has been the surface of choice. The three As dimer motif, shown in Figure 5, was first identified by Pashley *et al.* (1988) and confirmed by Biegelsen *et al.* (1990a) for the (2x4)/c(2x8) structure. Subsequently, several authors (Biegelsen *et al.*, 1989; Bressler-Hill *et al.*, 1992; Heller and Lagally, 1992; Xu *et al.*, 1993) observed a (2x4) unit cell with only two As dimers, which also is compatible with the principle of autocompensation if, e.g., the exposed Ga atoms in the second layer are dimerized, as predicted by total energy calculations (Northrup and Froyen, 1993). Unlike GaAs(110), however, changing the bias to inject charge into empty states in the semiconductor does not image the Ga species in the second layer (Wassermeier *et al.*, 1992), presumably because the rehybridization of the surface state bands predicted by Principle (5) renders the As empty states more accessible to the tunneling electrons from the tip. This issue is not resolved at the present time, however, because neither a quantitative structure calculation of the surface-state excitation spectra nor a quantitative struc-

ture analysis of the surface atomic geometry has been given.

On the basis of STM images, geometries for the sequence of distinct surface structures which appear on GaAs(100) as a function of surface composition were proposed by Biegelsen *et al.* (1990a). All of them satisfy the autocompensation Principle (4) but the relaxation and rehybridizations were not proposed. The second of these, besides the c(2x8) structure shown in Figure 5, which has been examined thoroughly by other groups, the proposed Ga rich c(8x2) structure, has been contested on the basis of high-resolution STM images by Skala *et al.* (1993). These authors argue for a structure consisting of chains of As dimers on a Ga substrate separated by two atomic rows of dimerized Ga atoms: a structure which also satisfies the autocompensation Principle (4). This sort of debate over which of the structures that satisfy Principle (4) are compatible with the STM images reveals the need for quantitative structure analyses using other techniques to specify definitively the surface atomic geometries. It also reveals the limitation of the autocompensation Principle (4) to predicting possible structures while requiring the surface state relaxation Principle (5) to determine which of these possible structures actually occurs.

### Synopsis

In this paper, we have argued that most, if not all, of the wide array of surface reconstructions observed on tetrahedrally coordinated semiconductors can be understood on the basis of five straightforward principles which capture the essence of the new types of chemical bonding which occur at their surfaces. It is useful to regard the uppermost few atomic layers of these surfaces as defining new chemical compounds epitaxially constrained to fit on the bulk substrate. The chemical principles governing bonding in these compounds are extensions of those familiar from bulk and molecular bonding. STM studies have made significant contributions to the development of these principles. The intent of this paper is to provide a brief overview of the principles themselves, an indication of STM contributions to them, and pointers to the literature so that readers can develop a more extensive understanding of these principles and use them to advantage in their daily research and teaching.

### Acknowledgement

The author is indebted to J. Boland and J. Kubby for sharing with him a draft of a detailed review of Scanning Tunneling Microscopy Studies of Semiconductor Surfaces which greatly assisted in the preparation of the section on STM.

## References

- Alerhand OL, Vanderbilt D, Meade RD, Joannopoulos JD (1988) Spontaneous formation of stress domains on crystal surfaces. *Phys Rev Lett* **61**: 1973-1988.
- Appelbaum JA, Baraff GA, Hamann DR (1976) GaAs (100): its spectrum, effective charge and reconstruction patterns. *Phys Rev B* **14**: 1623-1632.
- Biegelsen DK, Bringans RD, Swartz LE (1989) Observations of epitaxial growth using scanning tunneling microscopy. *SPIE Proceedings* **1168**: 136-143.
- Biegelsen DK, Bringans RD, Northrup JE, Swartz LE (1990a) Surface reconstructions of GaAs(100) observed by scanning tunneling microscopy. *Phys Rev B* **41**: 5701-5706.
- Biegelsen DK, Bringans RD, Northrup JE, Swartz LE (1990b) Reconstructions of GaAs(111) surfaces observed by scanning tunneling microscopy. *Phys Rev Lett* **65**: 452-455.
- Binnig G, Rohrer H, Gerber Ch, Wiebel E (1983) 7x7 Reconstruction on Si(111) resolved in real space. *Phys Rev Lett* **50**: 120-123.
- Bohr J, Fiedenhans'l R, Nielsen M, Toney M, Johnson RL, Robinson IK (1985) Model-independent structure determination of the InSb(111) 2x2 surface with use of synchrotron X-Ray diffraction. *Phys Rev Lett* **54**: 1275-1279.
- Bressler-Hill VM, Wassermeier K, Pond R, Maboudian GAD, Briggs P, Petroff M, Weinberg WH (1992) Atom resolved imaging and spectroscopy on the GaAs(001) surface using tunneling microscopy. *J Vac Sci Technol B* **10**: 1881-1885.
- Brommer KD, Needels M, Larson BE, Joannopoulos JD (1992) Ab initio theory of the Si(111)-(7x7) surface reconstruction: a challenge for massively parallel computation. *Phys Rev Lett* **68**: 1355-1358.
- Chadi DJ (1979a) Atomic and electronic structures of reconstructed Si(100) surfaces. *Phys Rev Lett* **43**: 43-47.
- Chadi DJ (1979b) (110) Surface atomic geometries of covalent and ionic semiconductors. *Phys Rev B* **19**: 2074-2082.
- Chadi DJ (1984) Vacancy induced reconstruction of the Ga(111) surface of GaAs. *Phys Rev Lett* **52**: 1911-1954.
- Chadi DJ (1989) Atomic structure of reconstructed group IV and III-V semiconductor surfaces. *Ultramicroscopy* **31**: 1-9.
- Chadi DJ (1991) Electron-hole counting rule at III-V surfaces: Applications to surface structure and passivation. In: *The Structure of Surfaces III*. Tong SY, Van Hove MA, Takayanagi K, Xie XD (eds.). Springer Series in Surface Sciences **24**. Springer-Verlag, Berlin. pp. 532-544.
- Dabrowski J, Scheffler M (1992) Self-consistent study of the electronic and structural properties of the clean Si(001)-(2x1) surface. *Appl Surf Sci* **56-58**: 15-19.
- Dassanayake UM, Chen W, Kahn A (1993) Atomic arrangement at the CuBr(100) surface and CuBr/GaAs(100) interface: Application of the electron counting method. *J Vac Sci Technol B* **11**: 1467-1471.
- Duke CB (1983) Surface structural chemistry of compound semiconductors. *J Vac Sci Technol B* **1**: 732-735.
- Duke CB (1987) Surface structural chemistry for microelectronics. In: *Atomic and Molecular Processing of Electronic and Ceramic Materials*. Aksay IA, McVay GL, Stroebe JT, Wagner JF (eds.). Materials Research Society, Pittsburgh. pp. 3-10.
- Duke CB (1988) Atomic geometry and electronic structure of tetrahedrally coordinated compound semiconductors. In: *Surface Properties of Electronic Materials*. King DA, Woodruff DP (eds.). The Chemical Physics of Solid Surfaces and Heterogeneous Catalysis **5**. Elsevier, Amsterdam. pp. 69-118.
- Duke CB (1992) Structure and bonding of tetrahedrally coordinated compound semiconductor cleavage faces. *J Vac Sci Technol A* **10**: 2032-2040.
- Duke CB (1993a) Surface structures of tetrahedrally coordinated semiconductors: Principles, practice and universality. *Appl Surf Sci* **65/66**: 543-552.
- Duke CB (1993b) Twenty years of semiconductor surface and interface structure determination and prediction. *J Vac Sci Technol B* **11**: 1336-1346.
- Duke CB, Wang YR (1988a) Mechanism and consequences of surface reconstruction on the cleavage faces of Wurtzite structure compound semiconductors. *J Vac Sci Technol A* **6**: 692-695.
- Duke CB, Wang YR (1988b) Surface structure and bonding of the cleavage faces of tetrahedrally coordinated II-VI compounds. *J Vac Sci Technol B* **6**: 1440-1442.
- Duke CB, Wang YR (1989) Surface atomic geometry and electronic structure of II-VI cleavage faces. *J Vac Sci Technol A* **7**: 2035-2038.
- Farrell HH, Harbison JP, Peterson LD (1987) Molecular beam epitaxy growth mechanisms on GaAs(001) surfaces. *J Vac Sci Technol B* **5**: 1482-1489.
- Feenstra RM, Stroscio JA (1987) Real-space determination of surface structure by scanning tunneling microscopy. *Physica Scripta* **T19**: 55-60.
- Feenstra RM, Thompson WA, Fein AP (1986) Real-space observation of  $\pi$ -bonded chains and surface disorder on Si(111) 2x1. *Phys Rev Lett* **56**: 608-611.
- Feenstra RM, Stroscio JA, Tersoff J, Fein AP (1987) Atom selective imaging of the GaAs(110) surface. *Phys Rev Lett* **58**: 1192-1195.
- Feidenhans'l R, Nielsen M, Grey F, Johnson RL,

Robinson IK (1987) X-ray determination of the GaSb (111)-(2x2) surface structure. *Surf Sci* **186**: 499-510.

Feidenhans'l R, Pedersen JS, Bohr J, Nielsen M (1988) Surface structure and long range order of the Ge (111)-(2x8) reconstruction. *Phys Rev B* **38**: 9715-9720.

Garcia A, Northrup JE (1993) Stress relief from alternately buckled dimers in Si(100). *Phys Rev B* **48**: 17350-17353.

Godin TJ, LaFemina JP, Duke CB (1992) Surface structure, bonding and dynamics: Universality of zincblende (110) potential energy surfaces. *J Vac Sci Technol A* **10**: 2059-2065.

Gray HB (1965) *Electrons and Chemical Bonding*. Benjamin, New York. pp. 155-175.

Hamers RJ, Tromp RM, Demuth JE (1986a) Surface electronic structure of Si(111)-(7x7) resolved in real space. *Phys Rev Lett* **18**: 1972-1975.

Hamers RJ, Tromp RM, Demuth JE (1986b) Scanning tunneling microscopy of Si(001). *Phys Rev B* **34**: 5343-5357.

Hamers RJ, Tromp RM, Demuth JE (1987) Electronic and geometric structure of Si(111)-(7x7) and Si(001) surfaces. *Surf Sci* **181**: 346-355.

Haneman D, Chernov AA (1989) Thermal conversion of the Si(111) 2x1 cleaved surface structure to the Si(111) 7x7 structure. *Surf Sci* **215**: 135-146.

Harrison WA (1979) Theory of polar surfaces. *J Vac Sci Technol* **16**: 1492-1496.

Heller EJ, Lagally MG (1992) *In situ* scanning tunneling microscopy observation of surface morphology of GaAs(001) grown by molecular beam epitaxy. *Appl Phys Lett* **60**: 2675-2679.

Ihm J, Cohen ML, Chadi DJ (1980) (2x1) reconstructed Si(001) surface: self-consistent calculations of dimer models. *Phys Rev B* **21**: 4592-4599.

Kahn A (1983) Semiconductor surface structures. *Surf Sci Repts* **3**: 193-300.

Kahn A (1994) Thirty years of atomic and electronic structure determination of surfaces of tetrahedrally coordinated compound semiconductors. *Surf Sci* **299/300**: 469-486.

Kochanski GP, Griffith JE (1991) A Ginzberg-Landau model for dimers on the Si(100) surface. *Surf Sci Lett* **249**: L293-L299.

Krüger P, Pollmann J (1993) *Ab initio* calculations of Si, As, S, Se and Cl adsorption on Si(001) surfaces. *Phys Rev B* **47**: 1898-1910.

Ludeke (1977) Sb-Induced surface states on (100) surfaces of III-V semiconductors. *Phys Rev Lett* **39**: 1042-1045.

MacLaren JM, Pendry JB, Rous PJ, Saldin DK, Somorjai GA, van Hove MA, Vvedensky DD (1987) *Surface Crystallographic Information Service: A Handbook of Surface Structures*. D. Reidel, Dordrecht.

352 pp.

Mailhot C, Duke CB, Chadi DJ (1985) Sb Overlayers on (110) Surfaces of III-V semiconductors, total energy minimization and surface electronic structure. *Phys Rev B* **31**: 2213-2229.

Needels M, Payne MC, Joannopoulos JD (1988) High order reconstructions of the Ge(100) surface. *Phys Rev B* **38**: 5543-5546.

Northrup JE (1993) Electronic structure of Si(100)c(4x2) calculated within the GW approximation. *Phys Rev B* **47**: 10032-10035.

Northrup JE, Cohen ML (1982) Reconstruction mechanism and surface state dispersion for Si(111)-(2x1). *Phys Rev Lett* **49**: 1349-1352.

Northrup JE, Froyen S (1993) Energetics of GaAs(100)-(2x4) and (4x2) reconstructions. *Phys Rev Lett* **71**: 2276-2279.

Pandey KC (1981) New  $\pi$ -bonded chain model for Si(111)-(2x1) surface. *Phys Rev Lett* **47**: 1913-1917.

Pandey KC (1982) Reconstruction of semiconductor surfaces. *Phys Rev Lett* **49**: 223-226.

Pashley MD (1989) Electron counting model and its application to island structures on molecular beam epitaxy grown GaAs(001) and ZnSe(001). *Phys Rev B* **40**: 10481-10487.

Pashley MD, Haberern KW (1991) Compensating surface defects induced by Si doping of GaAs. *Phys Rev Lett* **67**: 2697-2700.

Pashley MD, Haberern KW, Friday W, Woodall JM, Kirchner PD (1988) Structure of GaAs(001) (2x4)-c(2x8) determined by scanning tunneling microscopy. *Phys Rev Lett* **60**: 2176-2179.

Pauling L (1960) *The Nature of the Chemical Bond*. Cornell Univ. Press, Ithaca. Third Edition. pp. 221-264.

Skala SL, Hubacek JS, Tucker JR, Lyding JW, Chou ST, Cheng K-Y (1993) Structure of GaAs(100) c(8x2) determined by scanning tunneling microscopy. *Phys Rev B* **48**: 9138-9141.

Stich I, Payne MC, King-Smith RD, Lin JS, Clarke LJ (1992) *Ab initio* total energy calculation for extremely large systems: Application to the Takayanagi reconstruction of Si(111). *Phys Rev Lett* **68**: 1351-1354.

Stroscio JA, Feenstra RM, Fein AP (1987) Imaging electronic surface states in real space on the Si(111) 2x1 surface. *J Vac Sci Technol A* **5**: 838-841.

Takayanagi K, Tanashiro Y, Takahashi S, Takahashi M (1985) Structure analysis of the Si(111)-(7x7) reconstructed surface by transmission electron diffraction. *Surf Sci* **164**: 367-392.

Tong SY, Xu G, Mei WN (1984) Vacancy buckling model for the (2x2) GaAs(111) surface. *Phys Rev Lett* **52**: 1693-1696.

Tromp RM, Hamers RJ, Demuth JE (1985) Si(001) Dimer structure observed with scanning tunneling

microscopy. *Phys Rev Lett* **55**: 1303-1306.

Tromp RM, Hamers RJ, Demuth JE (1986) Atomic and electronic contributions to Si(111)-(7x7) scanning-tunneling-microscopy images. *Phys Rev B* **15**: 1388-1391.

Uhrberg RIG, Hanson GV (1991) Electronic structure of silicon surfaces: clean and ordered overlayers. *Crit Rev Solid State Mater Sci* **17**: 133-186.

Wassermeier M, Bressler-Hill V, Maboudian R, Pond K, Wang XS, Weinberg WH, Petroff PM (1992) Scanning tunneling microscopy of filled and empty arsenic states on the GaAs(001)-(2x4) surface. *Surf Sci Lett* **278**: L147-L151.

Weakliem PC, Smith GW, Carter EA (1990) Sub-picosecond interconversion of buckled and symmetric dimers on Si(100). *Surf Sci Lett* **232**: L219-L223.

Wolkow RA (1992) Direct observation of increase in buckled dimers on Si(100) at low temperature. *Phys Rev Lett* **68**: 2636-2639.

Whitman LJ, Stroscio JA, Dragoset RA, Celotta RJ (1990) Scanning-tunneling-microscopy study of InSb(110). *Phys Rev B* **42**: 7288-7291.

Xu G, Hu WY, Puga MW, Tong SY, Yeh JL, Wang SR, Lee BW (1985) Atomic geometry of the (2x2) GaP(111) surface. *Phys Rev B* **32**: 8473-8476.

Xu H, Hashizume T, Sakurai T (1993) GaAs(100) (2x4) Surface study by molecular beam epitaxy and field-ion scanning tunneling microscopy. *Jpn J Appl Phys* **32**: 1511-1514.

Yin MT, Cohen ML (1981) Theoretical determination of surface atomic geometry: Si(100)-(2x1). *Phys Rev B* **24**: 2303-2306.

**Editor's Note:** All of the reviewer's concerns were appropriately addressed by text changes, hence there is no **Discussion with Reviewers**.